A New Class of Electron-Rich Unsaturated Molecules: $Ru_2H_nX_{4-n}(P^iPr_3)_4$, X = Anion

Joseph N. Coalter, III, John C. Huffman, William E. Streib, and Kenneth G. Caulton*

Department of Chemistry and Molecular Structure Center, Indiana University, Bloomington, Indiana 47405-7102

Received September 17, 1999

Synthesis, spectroscopic, and X-ray structural characterization of $Ru_2H_nCl_{4-n}L_4$ (n = 2, 3) and $Ru_2H_2F_2L_4$ (L = P^iPr_3) are reported. The structure of $Ru_2HCl_3L_4$ is also reported. These are dinuclear species containing two five-coordinate, approximately square-pyramidal metal atoms. Halides, not hydrides, preferentially occupy bridging sites, and the $RuXL_2$ terminal moiety shows limited fluxionality, but hydrides do not migrate between metals. The limited steric protection provided by P^iPr_3 is evident from the dimerization observed and from the fact that all these structures have rather small ∠P−Ru−P (∼105°). Also reported are $RuHXL_2$ species with X = acetylacetonate, phenoxide, O_3SCH_3, and O_3SCF_3. Several examples of coordinated olefin to complexed carbene conversions are used to test the influence of anion X on reactivity.

We recently reported[1] the dehydrohalogenation of $Ru(H)_2Cl_2L_2$ (L = P^iPr_3) according to eq 1. Spectroscopic data on this

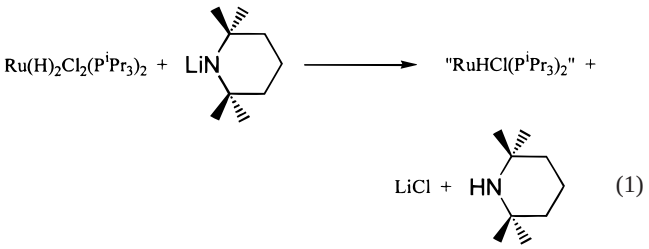

(1)

species were consistent with a nonplanar monomer that was isoelectronic with two 14-electron complexes we had recently characterized:[2,3] $RuH(CO)L_2^+$ and $RuPh(CO)L_2^+$. We have now grown diffraction-quality crystals of "$RuHClL_2$", and we report here the *dimeric* character of this compound and thus correct our previous error. This synthetic route also enables synthesis of $Ru_2H_nCl_{4-n}L_4$, with n = 1 and 3, whose structure we report, together with that of $[RuHFL_2]_2$. This fluoride compound is decisive in proving the retention of dimeric character in arene and ethereal solvents. Finally, we report the relationship of these dimers to products resulting from the halide metathesis reaction of $[RuHClL_2]_2$ with $TlOC_6H_5$, as well as products where the anion is acetylacetonate, O_3SCH_3, and O_3SCF_3.

Experimental Section

General Considerations. All manipulations were performed using standard Schlenk techniques or in an argon-filled glovebox unless otherwise noted. Solvents were distilled from Na/benzophenone or CaH_2, degassed prior to use, and stored in airtight vessels. $RuH_2Cl_2(P^iPr_3)_2$[4] and neopentyllithium[5] were prepared as previously reported, and anhydrous NMe_4F was used as received from Aldrich. ^1H NMR chemical shifts are reported in ppm relative to protio impurities in the deutero solvents. ^{31}P and ^{19}F NMR spectra are referenced to external standards of 85% H_3PO_4 and $CFCl_3$, respectively (both at 0 ppm). NMR spectra were recorded with either a Varian Gemini 2000 (300 MHz ^1H; 121 MHz ^{31}P; 75 MHz ^{13}C; 282 MHz ^{19}F) or a Varian Unity Inova instrument (400 MHz ^1H; 162 MHz ^{31}P; 101 MHz ^{13}C; 376 MHz ^{19}F).

$[RuHCl(P^iPr_3)_2]_2$. Under argon, 750 mg (1.64 mmol) of $RuH_2Cl_2(P^iPr_3)_2$ was slurried in 30 mL of toluene. Via dropping funnel, 230 mg (1.64 mmol) of lithium 2,2,6,6-tetramethylpiperidide in 20 mL of toluene was then added dropwise over 2 h and the mixture stirred overnight. The red solution was filtered through a medium porosity frit, and the solvent was then removed to a liquid N_2 trap. The deep-red product was dried overnight *in vacuo* to yield 510 mg of $[RuHCl(P^iPr_3)_2]_2$ (73%). The compound can be heated mildly (55 °C) to remove the free amine generated and can also be washed with small portions of cold (−78 °C) ether or hexane if necessary. Occasionally, a minor impurity (ca. 5%) of less soluble $Ru_2H_3Cl(P^iPr_3)_4$ is observed, which may be removed by selective crystallization from a pentane or toluene solution. ^1H NMR (400 MHz, C_6D_6, 20 °C): δ −24.2 (t, $^2J_{P-H}$ = 32.8 Hz, Ru-*H*), 1.34 (dvt, $J_{P-H} = {}^3J_{H-H}$ = 6.2 Hz, 18H, $P(CHMe_2)_3$), 1.36 (dvt, $J_{P-H} = {}^3J_{H-H}$ = 6.2 Hz, 18H, $P(CHMe_2)_3$), 2.19 (m, 6H, $P(CHMe_2)_3$). $^{31}P\{^1H\}$ NMR (162 MHz, C_6D_6, 20 °C): δ 84.1 (s). $^{13}C\{^1H\}$ NMR (75 MHz, C_6D_6, 20 °C): δ 20.8 (s, $P(CHMe_2)_3$), 21.2 (s, $P(CHMe_2)_3$), 28.4 (vt, J_{P-C} = 6.4 Hz, $P(CHMe_2)_3$).

$[RuHF(P^iPr_3)_2]_2$. Under argon, 1.00 g $[RuHCl(P^iPr_3)_2]_2$ (1.09 mmol) and 0.60 g anhydrous $[NMe_4]F$ (6.44 mmol) were stirred in benzene overnight. The benzene solubles were then transferred via cannula to a clean flask charged with 0.30 g of $[NMe_4]F$ (3.22 mmol). After the mixture was stirred overnight again, the solvent was removed in vacuo and the product was extracted twice with pentane. The pentane was then removed to a liquid N_2 trap to a yield a red solid that was dried *in vacuo*. Product prepared in this manner was found by ^1H, ^{31}P, and ^{19}F NMR spectroscopy to be approximately 80% $[RuHF(P^iPr_3)_2]_2$ and 20% $Ru_2H_2Cl(F)(P^iPr_3)_4$, a dimer with one fluoride and one chloride bridging (see below). $[RuHF(P^iPr_3)_2]_2$ can be prepared in greater than 95% purity with additional halide exchange cycles. Yield: 725 mg. ^1H NMR (400 MHz, THF-d_8/Et_2O-d_{10} (1:3), 25 °C): δ −28.2 (tt, 1H, $^2J_{H-P}$ = 39 Hz, $^2J_{H-F}$ = 8 Hz, Ru-*H*), 1.23 (dvt, 18H, $J_{H-P} = J_{H-H}$ = 5 Hz, $P(CHMe_2)_3$), 1.29 (dvt, 18H, $J_{H-P} = J_{H-H}$ = 5 Hz, $P(CHMe_2)_3$), 2.02 (m, 6H, $P(CHMe_2)_3$). $^{31}P\{^1H\}$ NMR (162 MHz, THF-d_8/Et_2O-d_{10} (1:3), 25 °C): δ 91.8 (t, $^2J_{P-F}$ = 66 Hz). ^{19}F NMR (376 MHz, THF-d_8/

* To whom correspondence should be addressed. E-mail: caulton@indiana.edu.

(1) Coalter, J. N.; Spivak, G. J.; Gerard, H.; Clot, E.; Davidson, E. R.; Eisenstein, O.; Caulton, K. G. *J. Am. Chem. Soc.* **1998**, *120*, 9388.
(2) Huang, D.; Streib, W. E.; Eisenstein, O.; Caulton, K. G. *Angew. Chem., Int. Ed. Engl.* **1997**, *36*, 2004.
(3) Huang, D.; Huffman, J. C.; Bollinger, J. C.; Eisenstein, O.; Caulton, K. G. *J. Am. Chem. Soc.* **1997**, *119*, 7398.
(4) Grünwald, C.; Gevert, O.; Wolf, J.; González-Herrero, P.; Werner, H. *Organometallics* **1996**, *15*, 1960−1962.
(5) Schrock, R. R.; Fellman, J. D. *J. Am. Chem. Soc.* **1978**, *100*, 3359.

10.1021/ic991112y CCC: $19.00
Published on Web 08/01/2000

Et_2O-d_{10} (1:3), 25 °C): δ −330.8 (apparent quintet, $^2J_{F-P}$ = 66 Hz; the $^{19}F-^1H$ coupling was not resolved). $^{13}C\{^1H\}$ NMR (101 MHz, THF-d_8/Et_2O-d_{10} (1:3), 25 °C): δ 20.8 (s, $P(CHMe_2)_3$), 20.9 (s, $P(CHMe_2)_3$), 27.5 (vt, J_{C-P} = 9 Hz, $P(CHMe_2)_3$).

$Ru_2H_2Cl(F)(P^iPr_3)_4$. In the halide exchange of $[RuHCl(P^iPr_3)_2]_2$ to give $[RuHF(P^iPr_3)_2]_2$, this species was observed after 30 min when the reaction was monitored by ^1H and ^{31}P spectroscopy, in addition to being present as specified above. ^1H NMR (400 MHz, THF-d_8/Et_2O-d_{10} (1:3), 25 °C): δ −26.6 (td, 1H, $^2J_{H-P}$ = 39 Hz, $^2J_{H-F}$ = 19 Hz, Ru-*H*). The signals for the P^iPr_3 ligands are masked by those of $[RuHF(P^iPr_3)_2]_2$. $^{31}P\{^1H\}$ NMR (162 MHz, THF-d_8/Et_2O-d_{10} (1:3), 25 °C): δ 90.5 (d, $^2J_{P-F}$ = 57 Hz). ^{19}F NMR (376 MHz, THF-d_8/Et_2O-d_{10} (1:3), 25 °C): δ −337.7 (poorly resolved quintet of doublets, $^2J_{F-P}$ = 57 Hz, $^2J_{F-H} \approx$ 15 Hz). $^{13}C\{^1H\}$ NMR (101 MHz, THF-d_8/Et_2O-d_{10} (1:3), 25 °C): δ 20.7 (s, $P(CHMe_2)_3$), 21.0 (s, $P(CHMe_2)_3$), 27.7 (vt, J_{C-P} = 10 Hz, $P(CHMe_2)_3$).

$Ru_2H_3Cl(P^iPr_3)_4$. Under argon, 1.90 g (3.8 mmol) of $RuH_2Cl_2(P^iPr_3)_2$ and 0.60 g (7.7 mmol) of neopentyllithium were added to a 100 mL Schlenk flask. A total of 40 mL of pentane was added, and the slurry was stirred overnight to yield a deep-purple solution. The solution was filtered, reduced to $^1/_3$ its volume in vacuo, and cooled to −40 °C to yield 200 mg of a dark-purple solid. The mother liquor was decanted, reduced again, and cooled to yield a second crop of product. Total combined yield after drying *in vacuo* was 350 mg. ^1H NMR (400 MHz, 25 °C, C_6D_6): δ 1.28 (dd, $^3J_{P-H}$ = 12 Hz, $^3J_{H-H}$ = 8 Hz, 6H, $P(CHMe_2)_3$), 2.24 (m, 1H, $P(CHMe_2)_3$). $^{31}P\{^1H\}$ NMR (162 MHz, 25 °C, C_6D_6): no signal seen because of peak broadness. $^{13}C\{^1H\}$ NMR (101 MHz, 25 °C, C_6D_6): δ 20.8 (s, $P(CHMe_2)_3$), 29.7 (d, $^2J_{P-C}$ = 10 Hz, $P(CHMe_2)_3$).

$Ru_2HCl_3(P^iPr_3)_4$. No viable synthetic preparation for this molecule has been found. The crystal obtained for X-ray analysis was a result of cocrystallization from a sample of $[RuHCl(P^iPr_3)_2]_2$. Since no NMR signals for this molecule are observed from analysis of bulk $[RuHCl(P^iPr_3)_2]_2$, it is assumed that $Ru_2HCl_3(P^iPr_3)_4$ is produced as a minute impurity in the preparation of $[RuHCl(P^iPr_3)_2]_2$.

(η^5-C_6H_5O)$RuH(P^iPr_3)_2$. TlOPh was prepared in quantitative yield by reaction of phenol with equimolar TlOEt in pentane. The TlOPh precipitate was then washed with pentane and dried in vacuo. Under Ar, 0.200 g (0.22 mmol) of $[RuHCl(P^iPr_3)_2]_2$ and 0.120 g (0.40 mmol) of TlOPh were combined in 25 mL of pentane. The reaction was stirred overnight at room temperature and allowed to stand for 1 h, and then the pentane solubles were collected via cannula. The pentane solution was concentrated to approximately $^1/_3$ its original volume and cooled to −78 °C. The red-brown precipitate was collected and dried *in vacuo* to yield 0.120 g of (η^5-C_6H_5O)$RuH(P^iPr_3)_2$ (54%, quantitative by ^{31}P NMR before workup). ^1H NMR (400 MHz, C_6D_6, 25 °C): δ −13.2 (t, 1H, $^2J_{H-P}$ = 37 Hz, Ru−*H*), 1.05 (dvt, 18H, J_{H-P} = 5 Hz, J_{H-H} = 7 Hz, $P(CHMe_2)_3$), 1.13 (dvt, 18H, J_{H-P} = 5 Hz, J_{H-H} = 7 Hz, $P(CHMe_2)_3$), 1.97(m, 6H, $P(CHMe_2)_3$), 3.97 (t, 1H, J_{H-H} = 5 Hz, p-C_6H_5O), 4.92 (d, 2H, J_{H-H} = 6 Hz, o-C_6H_5O), 5.38 (apparent t, 2H, J_{H-H} = 6 Hz, m-C_6H_5O). $^{31}P\{^1H\}$ NMR (162 MHz, C_6D_6, 25 °C): δ 65.0 (s). $^{13}C\{^1H\}$ NMR (101 MHz, C_6D_6, 25 °C): δ 20.7 (s, $P(CHMe_2)_3$), 21.0 (s, $P(CHMe_2)_3$), 28.5 (vt, J_{P-C} = 9 Hz, $P(CHMe_2)_3$), 69.0 (s, p-C_6H_5O), 81.1 (s, o-C_6H_5O), 95.1 (s, m-C_6H_5O), 166.1 (s, carbonyl/ipso-C_6H_5O).

$RuHF(P^iPr_3)_2$(=C(Me)OEt). Under argon, 20 mg (0.023 mmol) of $[RuHF(P^iPr_3)_2]_2$ was dissolved in 0.5 mL of C_6H_6 in an NMR tube equipped with a Teflon seal. Via syringe, 8.6 μL (0.046 mmol) of ethyl vinyl ether was added, and the tube is sealed. After 24 h of agitation, the volatiles were removed *in vacuo* and the residue is dissolved in C_6D_6. ^1H and $^{31}P\{^1H\}$ NMR reveal formation of $RuHF(CO)(P^iPr_3)_2$ (60%) in addition to $RuHF(P^iPr_3)_2$(=C(Me)OEt) (40%). The P^iPr_3 proton signals of both products overlap substantially. ^1H NMR (400 MHz, C_6D_6, 20 °C): δ −25.8 (broad apparent quartet, $^2J_{P-H}$ = $^2J_{F-H}$ = 16 Hz, 1 H, Ru*H*), 1.18 (t, J_{H-H} = 7 Hz, 3H, Ru=C(Me)OCH_2CH_3), 1.20 (dvt, J_{P-H} = $^3J_{H-H}$ = 6 Hz, 18H, $P(CHMe_2)_3$), 1.25 (dvt, J_{P-H} = $^3J_{H-H}$ = 6 Hz, 18H, $P(CHMe_2)_3$), 2.28 (m, 6H, $P(CHMe_2)_3$), 2.66 (s, 3H, Ru=C(*Me*)OEt), 4.52 (q, J_{H-H} = 7 Hz, 2H, Ru=C(Me)OCH_2CH_3). $^{31}P\{^1H\}$ NMR (162 MHz, C_6D_6, 20 °C): δ 57.8 (d, $^2J_{F-P}$ = 24 Hz). ^{19}F NMR (376 MHz, C_6D_6, 20 °C): δ −227.6 (t, broad, partially resolved).

$[RuH(OSO_2Me)(P^iPr_3)_2]_x$. Under argon, 10 mg (0.011 mmol) of $[RuHF(P^iPr_3)_2]_2$ was dissolved in 0.5 mL of C_6D_6 in an NMR tube. Via syringe, 3.5 μL (0.023 mmol) of trimethylsilyl methanesulfonate was added and the tube shaken. ^1H and $^{31}P\{^1H\}$ NMR spectra taken after 10 min reveal complete conversion to $[RuH(OSO_2Me)(P^iPr_3)_2]_x$. The only fluorine-containing product observed by ^{19}F NMR is trimethylsilyl fluoride (−160 ppm, septet). A small amount (ca. 5%) of $[(C_6D_6)RuH(P^iPr_3)_2][OSO_2Me]$ (^1H NMR, −11.2 ppm, t, $^2J_{P-H}$ = 43 Hz, Ru*H*; $^{31}P\{^1H\}$ NMR, 62.6 ppm) is also detected after this elapsed time. ^1H NMR (400 MHz, C_6D_6, 20 °C): δ −30.1 (t, $^2J_{P-H}$ = 36 Hz, 1H, Ru-*H*), 1.14 (dvt, J_{P-H} = $^3J_{H-H}$ = 6 Hz, 18H, $P(CHMe_2)_3$), 1.19 (dvt, J_{P-H} = $^3J_{H-H}$ = 6 Hz, 18H, $P(CHMe_2)_3$), 1.90 (m, 6H, $P(CHMe_2)_3$), 2.69 (broad s, 3H, OSO_2Me). $^{31}P\{^1H\}$ NMR (162 MHz, C_6D_6, 20 °C): δ 89.6 (s).

$RuH(OSO_2Me)(P^iPr_3)_2$(=C(Me)OEt). Under argon, 15 mg (0.017 mmol) of $[RuHF(P^iPr_3)_2]_2$ was dissolved in 0.5 mL of C_6D_6 in an NMR tube. Via syringe, 5.3 μL (0.034 mmol) of trimethylsilyl methanesulfonate was added and the tube shaken. After 10 min, 6.5 μL (0.068 mmol) of ethyl vinyl ether was added via syringe. ^1H and $^{31}P\{^1H\}$ NMR spectra taken after 15 min revealed virtually quantitative formation of $RuH(OSO_2Me)(P^iPr_3)_2$(=C(Me)OEt) plus signals for trimethylsilyl fluoride and the excess ethyl vinyl ether. ^1H NMR (400 MHz, C_6D_6, 20 °C): δ −22.8 (broad s, 1 H, Ru*H*), 1.08 (t, J_{H-H} = 7 Hz, 3H, Ru=C(Me)OCH_2CH_3), 1.16 (dvt, J_{P-H} = $^3J_{H-H}$ = 6 Hz, 18H, $P(CHMe_2)_3$), 1.31 (dvt, J_{P-H} = $^3J_{H-H}$ = 6 Hz, 18H, $P(CHMe_2)_3$), 2.41 (m, 6H, $P(CHMe_2)_3$), 2.54 (s, 3H, Ru=C(*Me*)OEt), 2.70 (broad s, 3H, OSO_2Me), 3.88 (q, J_{H-H} = 7 Hz, 2H, Ru=C(Me)OCH_2CH_3). $^{31}P\{^1H\}$ NMR (162 MHz, C_6D_6, 20 °C): δ 54.6 (s).

$RuH(acac)(P^iPr_3)_2$. Under argon, 100 mg (0.112 mmol) of $[RuHF(P^iPr_3)_2]_2$ was dissolved in 20 mL of benzene and, via syringe, 42.6 μL (0.225 mmol) of 2-trimethylsiloxypent-2-ene-4-one was added to the stirred solution. After 2 h, the volatiles were removed to give an orange powder that was isolated in quantitative yield after drying *in vacuo*. ^1H NMR (400 MHz, C_6D_6, 20 °C): δ −26.6 (t, $^2J_{P-H}$ = 36.4 Hz, 1 H, Ru*H*), 1.25 (dvt, J_{P-H} = $^3J_{H-H}$ = 8 Hz, 18H, $P(CHMe_2)_3$), 1.32 (dvt, J_{P-H} = $^3J_{H-H}$ = 8 Hz, 18H, $P(CHMe_2)_3$), 1.89 (s, 6H, $(CH_3C(=O))_2CH$), 2.22 (m, 6H, $P(CHMe_2)_3$), 5.45 (s, 1H, $(CH_3C(=O))_2CH$). $^{31}P\{^1H\}$ NMR (162 MHz, C_6D_6, 20 °C): δ 80.9 (s). $^{13}C\{^1H\}$ NMR (101 MHz, C_6D_6, 20 °C): δ 20.5 (s, $P(CHMe_2)_3$), 20.6 (s, $P(CHMe_2)_3$), 26.7 (vt, J_{P-C} = 8.5 Hz, $P(CHMe_2)_3$), 27.6 (s, $(CH_3C(=O))_2CH$), 99.9 (s, $(CH_3C(=O))_2CH$), 185.1 (s, $(CH_3C(=O))_2CH$).

$RuH(acac)(P^iPr_3)_2$(=C(Me)OEt). Under argon, 20 mg (0.038 mmol) of $RuH(acac)(P^iPr_3)_2$ was dissolved in 0.5 mL of C_6D_6 in an NMR tube equipped with a Teflon closure. Via syringe, 4.0 μL (0.042 mmol) of ethyl vinyl ether was added and the tube sealed and agitated. NMR spectra taken after 24 h show clean conversion to $RuH(acac)(P^iPr_3)_2$(=C(Me)OEt). ^1H NMR (400 MHz, C_6D_6, 20 °C): δ −18.7 (t, $^2J_{P-H}$ = 25.2 Hz, 1 H, Ru*H*), 1.13 (t, J_{H-H} = 7 Hz, 3H, Ru=C(Me)OCH_2CH_3), 1.30 (dvt, J_{P-H} = $^3J_{H-H}$ = 6 Hz, 18H, $P(CHMe_2)_3$), 1.34 (dvt, J_{P-H} = $^3J_{H-H}$ = 6 Hz, 18H, $P(CHMe_2)_3$), 1.81 (s, 3H, $(CH_3C(=O))_2CH$), 2.02 (s, 3H, $(CH_3C(=O))_2CH$), 2.05 (broad m, 6H, $P(CHMe_2)_3$), 2.59 (s, 3H, Ru=C(*Me*)OEt), 3.65 (q, J_{H-H} = 7 Hz, 2H, Ru=C(Me)OCH_2CH_3), 5.39 (s, 1H, $(CH_3C(=O))_2CH$). $^{31}P\{^1H\}$ NMR (162 MHz, C_6D_6, 20 °C): δ 55.9 (s). $^{13}C\{^1H\}$ NMR (101 MHz, C_6D_6, 20 °C): δ 15.1 (s, Ru=C(Me)OCH_2CH_3), 19.7 (s, $P(CHMe_2)_3$), 20.4 (s, $P(CHMe_2)_3$), 25.7 (vt, J_{P-C} = 7.9 Hz, $P(CHMe_2)_3$), 28.6 (s, $(CH_3C(=O))_2CH$), 29.6 (s, $(CH_3C(=O))_2CH$), 34.6 (s, Ru=C(*Me*)OEt), 64.8 (s, Ru=C(Me)OCH_2CH_3), 99.7 (s, $(CH_3C(=O))_2CH$), 186.1 (s, $(CH_3C(=O))_2CH$), 188.2 (s, $(CH_3C(=O))_2CH$), 300.9 (broad t, Ru=*C*).

$[(\eta^6$-$C_6H_6)RuH(P^iPr_3)_2][OTf]$. Under argon, 150 mg (0.163 mmol) of $[RuHClL_2]_2$ was dissolved in 25 mL of benzene, and 66 μL (0.330 mmol) of trimethylsilyl trifluoromethanesulfonate was added to the stirred solution. After 1 h, a dark precipitate had formed and the solvent was removed to a liquid N_2 trap. The solid was then washed with pentane (3 × 10 mL) and dried *in vacuo* to yield a bright-yellow powder (172 mg). ^1H NMR (400 MHz, CD_2Cl_2, 20 °C): δ −10.4 (t, 43.6 Hz, 1 H, Ru*H*), 1.25 (dvt, J_{P-H} = $^3J_{H-H}$ = 7 Hz, 18H, $P(CHMe_2)_3$), 1.28 (dvt, J_{P-H} = $^3J_{H-H}$ = 7 Hz, 18H, $P(CHMe_2)_3$), 2.04 (m, 6H, $P(CHMe_2)_3$), 5.88 (s, 6H, η^6-C_6H_6). $^{31}P\{^1H\}$ NMR (162 MHz, CD_2Cl_2, 20 °C): δ 62.8 (s). Anal. Calc (found) for $C_{25}H_{49}F_3O_3P_2RuS$: C, 46.21 (46.08); H, 7.60 (7.22).

Table 1. Crystallographic Data

	$[RuHF(P^iPr_3)_2]_2$	$[RuHCl(P^iPr_3)_2]_2$	$Ru_2HCl_3(P^iPr_3)_4$	$Ru_2H_3Cl(P^iPr_3)_4$
formula	$C_{36}H_{86}F_2P_4Ru_2$	$C_{35}H_{86}Cl_2P_4Ru_2$	$C_{36}H_{85}Cl_3P_4Ru_2$	$C_{36}H_{87}ClP_4Ru_2$
a, Å	13.750(1)	17.155(8)	13.403(8)	13.659(6)
b, Å	15.989(2)	19.934(8)	18.805(12)	16.671(6)
c, Å	11.023(1)	14.204(6)	36.460(25)	11.757(4)
α, Å	105.63(0)	90.13(2)		100.67(2)
β, Å	110.83(0)	101.90(2)		104.44(1)
γ, Å	86.14(0)	73.13(2)		106.11(1)
V, Å^3	2180.3(7)	4539.75	9189.72	2396.05
Z	2	4	8	2
fw	883.11	916.02	949.46	927.64
space group	$P\bar{1}$	$P\bar{1}$	Pbca	$P\bar{1}$
temp, °C	−171	−171	−165	−172
λ, Å	0.710 69	0.710 69	0.710 69	0.710 69
ρ_{cald}, g/cm^{-3}	1.345	1.340	1.373	1.286
μ(Mo K$_a$), cm^{-1}	8.7	9.5	9.9	8.4
R^a	0.0301	0.1048	0.0673	0.0616
$R_w{}^b$	0.0317	0.0957	0.0430	0.0477

[a] $R = \sum||F_o| - |F_c||/\sum|F_o|$. [b] $R_w = [\sum w(|F_o| - |F_c|)^2/\sum w|F_o|^2]^{1/2}$ where $w = (1/\sigma^2)(|F_o|)$.

X-ray Structure Determination of $[RuHCl(P^iPr_3)_2]_2$. All crystals studied were mounted under inert gas using silicone grease and then transferred to a goniostat and cooled to −171 °C for characterization and data collection (6° < 22° < 45°) (see Table 1). A preliminary search for peaks followed by analysis using programs DIRAX and TRACER revealed a triclinic cell. The solution of the structure established the space group as $P\bar{1}$. Of 11 924 unique intensities, only 4582 (38%) were considered observed by the criterion $I \geq 2\sigma(I)$. Four standards collected every 300 data showed a small but acceptable drift in the data, and no correction was applied. No correction for absorption was needed (μ = 9.47 cm^{-1}, μd_{mid} = 0.02). The structure was solved using a combination of direct methods (MULTAN78) and Fourier techniques. The positions of the four Ru atoms in the asymmetric unit were obtained from an initial E-map. The remaining nonhydrogen atoms that were located were obtained from iterations of a least-squares refinement followed by a difference Fourier calculation. Disorder was found in some of the ^{i}Pr groups, and these were modeled in a conventional manner with isotropic thermal parameters. Anticipated H's on the Ru's were not observed and were not included in the refinements. In the final cycles of refinement, all nonhydrogen atoms not excluded above were varied with anisotropic thermal parameters that, with the isotropic atoms and an extinction and scale parameter, gave a total of 716 variables. The largest peak in the final difference map was 2.2 e/Å^3 located 1.9 Å from C(80), and the deepest hole was −1.5 e/Å^3.

X-ray Structure Determination of $[RuHF(P^iPr_3)_2]_2$. The crystal possessed no symmetry or systematic absences, indicating a triclinic space group (Table 1). Subsequent solution and refinement confirmed the centrosymmetric choice. The data were collected (6° < 22 < 50°) and equivalent reflections averaged after an absorption correction. The structure was readily solved using direct methods (MULTAN78) and Fourier techniques. Hydrogen atoms, including the two hydrides, were located in difference Fourier maps phased on the nonhydrogen atoms and were refined isotropically in the final cycles of refinement. A final difference Fourier was featureless, the largest peak of intensity 1.40 e/Å^3 lying at the Ru(2) metal site.

X-ray Structure Determination of $Ru_2H_3Cl(P^iPr_3)_4$. The crystal possessed no symmetry or systematic absences, corresponding to one of the triclinic space groups. Subsequent solution and refinement confirmed the centrosymmetric choice, $P\bar{1}$ (Table 1). Equivalent reflections (6° < 2θ < 50°) were averaged after correction for absorption. The structure was readily solved using direct methods (MULTAN78) and Fourier techniques. Nonhydride hydrogen atoms were readily located in a difference Fourier map phased on the nonhydrogen atoms. Hydrogen atoms were placed in fixed idealized positions for the final cycles of refinement. Three peaks located in a difference Fourier lie in positions expected for the anticipated hydrides and are included as H(A), H(B), and H(C) but not refined. There is a disordered toluene molecule present at a center of inversion in the cell. A final difference Fourier was featureless, the largest peak being of intensity 1.40 e/Å^3 and lying at one of the metal sites.

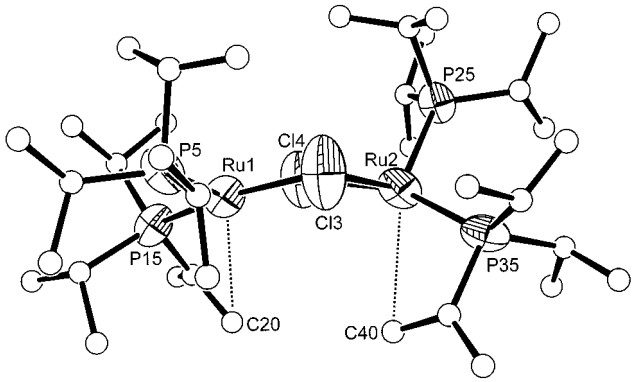

Figure 1. ORTEP drawing of the nonhydrogen atoms of $[RuHCl(P^iPr_3)_2]_2$, showing selected atom labeling. The short Ru−CH$_3$ contacts are shown to C20 (3.57 Å) and C40 (3.08 Å).

X-ray Structure Determination of $Ru_2HCl_3(P^iPr_3)_4$. The crystal chosen possessed orthorhombic symmetry (Table 1) with systematic absences corresponding to the unique space group *Pbca*. Subsequent solution and refinement confirmed this choice. Data (6° < 2θ < 50°) were corrected for absorption, and equivalent reflections were then averaged. The structure was solved using direct methods (SHELXTL) and Fourier techniques. Hydrogen atoms were included as fixed isotropic contributors in the final cycles of refinement. It was not possible to identify any hydrides associated with the metal atoms, although there is ample room on both metals. A final difference Fourier was featureless, the largest peaks (1.12 e/Å^3) lying in the vicinity of the metal atoms.

Results

Syntheses. The general synthetic method relies on dehydrohalogenation of the unusual (Ru^{IV}, unsaturated) $Ru(H)_2Cl_2L_2$ (L = P^iPr_3), using a strong amide base, or (for $Ru_2H_3ClL_4$) $LiCH_2CMe_3$, in stoichiometric amount. The products are hydrocarbon-soluble but highly reactive species that are handled under argon.

$[RuHCl(P^iPr_3)_2]_2$. The unit cell of $[RuHClL_2]_2$ contains two independent molecules. This is advantageous in that unexpected structural features, if they appear in both molecules, can be concluded to reveal real intramolecular preferences, and they may also be useful in deducing the hydride location, which will not be directly detected in the diffraction data.

In the two molecules (Figure 1 and Table 2), the Ru_2Cl_2 quadrilaterals differ insignificantly and the Ru−Cl bond lengths and the bond angles show no difference in the two metals in the ring. However, the two metals in any one molecule are

Table 2. Selected Bond Distances (Å) and Angles (deg) for $[RuHCl(P^iPr_3)_2]_2$

		molecule A	molecule B
Ru(1)	Cl(3)	2.428(8)	2.454(8)
Ru(1)	Cl(4)	2.448(6)	2.453(6)
Ru(1)	P(5)	2.255(6)	2.252(6)
Ru(1)	P(15)	2.268(7)	2.254(7)
Ru(2)	Cl(3)	2.443(7)	2.450(6)
Ru(2)	Cl(4)	2.442(7)	2.443(7)
Ru(2)	P(25)	2.201(6)	2.189(6)
Ru(2)	P(35)	2.273(7)	2.236(7)

			molecule A	molecule B
Cl(3)	Ru(1)	Cl(4)	78.67(22)	79.94(22)
Cl(3)	Ru(1)	P(5)	87.74(24)	87.88(23)
Cl(3)	Ru(1)	P(15)	167.01(24)	166.57(22)
Cl(4)	Ru(1)	P(5)	156.11(26)	160.86(25)
Cl(4)	Ru(1)	P(15)	89.86(22)	87.85(22)
P(5)	Ru(1)	P(15)	105.10(24)	105.34(24)
Cl(3)	Ru(2)	Cl(4)	78.50(22)	80.23(23)
Cl(3)	Ru(2)	P(25)	115.8(3)	117.77(25)
Cl(3)	Ru(2)	P(35)	98.93(24)	97.69(25)
Cl(4)	Ru(2)	P(25)	93.39(23)	93.12(23)
Cl(4)	Ru(2)	P(35)	160.06(25)	159.64(23)
P(25)	Ru(2)	P(35)	105.32(24)	105.53(23)
Ru(1)	Cl(3)	Ru(2)	99.39(25)	96.46(26)
Ru(1)	Cl(4)	Ru(2)	98.88(22)	96.66(24)

differentiated with regard to their two phosphine ligands. Ru1 and Ru46 (molecules A and B, respectively) have four essentially coplanar ligands, while Ru2 and Ru45 (molecules A and B) do not have their attached two Cl and two P in a plane. The relevant angles are shown in **A**. Moreover, Ru2−P25 and

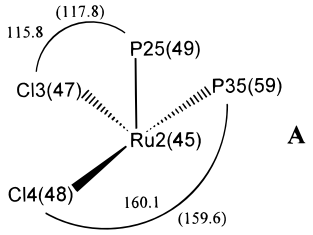

A

Ru45−P49 distances, involving the phosphorus atom not in the Ru_2Cl_2 plane, are 5−8 esd's shorter (∼2.19 Å) than the other Ru−P distances (∼2.24−2.27 Å). One possible interpretation is that both hydrides are on the planar-coordinated Ru atom (**I**), while an alternative is **II**. *Both* dimers show all four ∠P−

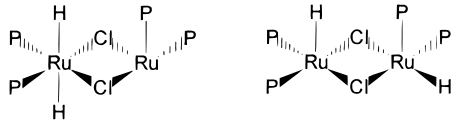

I **II**

Ru−P in the very small range 105.1(2)−105.5(2) Å. This is, moreover, a very small angle for a phosphine as bulky as P^iPr_3, which normally occupies mutually *trans* sites. The in-plane phosphorus atoms on the nonplanar-coordinated metal (i.e., P35 and P59) each have one ^{i}Pr group with an unusually small ∠Ru−P−C(quaternary). This angle (100−101°) is 6°−10° smaller than the smallest angle on the other phosphines, and in each case, this ^{i}Pr group is directed closer to Ru at the site *trans* to the out-of-plane phosphorus, P25 or P49. The resulting shortest Ru−C distances are 3.08 (Ru2/C40) and 3.12 (Ru45/C61) Å for the two independent molecules. This is a very weak agostic interaction or it represents only "tucking" one ^{i}Pr into an available void, to minimize phosphine−phosphine repulsion. However, this contact does indicate that a hydride *cannot* be in this site trans to P25 and P49. The Ru/Ru separation is 3.71 Å, and thus nonbonding.

$[RuHFL_2]_2$. This compound was synthesized by twice treating $[RuHClL_2]_2$ with excess anhydrous $[NMe_4]F$ in benzene. The ^{1}H NMR spectrum in benzene-d_6 at 25 °C shows a hydride triplet of triplets due to coupling to two phosphines and *two* fluorines. This latter coupling is the first evidence that the molecule is a dimer $[L_2RuH(\mu\text{-}F)]_2$. The $^{31}P\{^1H\}$ NMR spectrum is a triplet, also indicating coupling to two (bridging) fluorines in the dimer. If the Cl → F replacement has not proceeded to completion, $L_4Ru_2H_2FCl$ is also observed as a hydride triplet of doublets and a $^{31}P\{^1H\}$ NMR doublet within 2 ppm of that of the difluoride. The magnitude of $^2J_{H-Ru-F}$ in the monofluoride (19 Hz) is markedly different from that in the difluoride (9.2 Hz). In 1:3 THF-d_8/Et_2O-d_{10}, chosen for low viscosity at low temperature, the ^{1}H and ^{31}P NMR chemical shifts are unchanged, showing that no bridge splitting or coordination occurs in these potential donor solvents. The ^{19}F NMR spectra of the mono- and of the difluoride each consist of a quintet far upfield (−338 ppm and −331 ppm), consistent with coupling to four equivalent ^{31}P nuclei (in the monofluoride, F−H coupling is also partially resolved). The NMR spectra of all three nuclei simply broaden as the temperature is reduced to −80 °C, but no decoalescence is achieved. The simple ^{19}F, ^{31}P, and ^{1}H NMR spectra at 25 °C require a site exchange process where the two phosphorus atoms on any Ru exchange positions, but the hydrides must stay (a) on the same metal and (b) on the same side of the $Ru_2(\mu\text{-}X)_2$ plane, the latter because, at 25 °C, one observes two ^{i}Pr methyl proton chemical shifts, indicating that they are diastereotopic. ^{1}H (hydride region), $^{31}P\{^1H\}$, and ^{19}F NMR spectra of a 4:1 mixture of $Ru_2H_2F_2L_4$/$Ru_2H_2FClL_4$ are shown in Figure 2.

Structure of $[RuHF(P^iPr_3)_2]_2$. Although the crystal is not isomorphous with the chloride analogue, it displays (Figure 3 and Table 3) all the characteristics of the chloride structure. The Ru_2F_2 unit has four equal sides, but the two metals have different locations for the phosphines. Although the phosphines have the same small ∠P−Ru−P (∼107°), Ru2 is not coplanar with two F and two P ligands, while Ru1 is in the plane of its two F and two P atoms. This lack of symmetry is a feature it shares with $[RuHCl(P^iPr_3)_2]_2$. As in the chloride, one ∠Ru2−P35−C36 angle is ∼9° smaller than is true in the other three phosphines. In this structure determination, the hydrides were located. They are both terminal and lie on the *same* side of the Ru_2F_2 plane. While the resulting coordination geometry at Ru1 is square-pyramidal with apical hydride, this is not true at Ru2, where the angles H−Ru−F differ greatly (98.6(1)° and 144.1(1)°; compare 102.7(1)° and 121.3(1)° for Ru1). The large H−Ru(2)−F4 angle creates the space where the small ∠Ru2−P35−C36 brings methyl group C38 closer to Ru2. The resulting Ru2−C38 distance is 3.28 Å. This is at best a very weak agostic interaction, but it occurs trans to the out-of-plane phosphine P25. As in the chloride, the Ru−P distance to the out-of-plane phosphorus is the shortest in the molecule. The Ru−Ru separation is 3.35 Å, again nonbonding in nature.

$Ru_2H_3Cl(P^iPr_3)_4$. This compound is formed by treating $RuH_2Cl_2(P^iPr_3)_2$ with either excess lithium 2,2,6,6-tetramethylpiperidide (LiTMP) or neopentyllithium in benzene or pentane. Though $[RuHCl(P^iPr_3)_2]_2$ is formed initially by dehydrohalogenation of $RuH_2Cl_2(P^iPr_3)_2$, the presence of extra base results in the isolation of $Ru_2H_3Cl(P^iPr_3)_4$, where the source of the two additional hydrogens (compared to a dimer of "$Ru(P^iPr_3)_2$" and $RuHCl(P^iPr_3)_2$) was not determined.

At room temperature in toluene-d_8, $Ru_2H_3Cl(P^iPr_3)_4$ shows only two signals for the phosphine ligands by ^{1}H NMR at δ

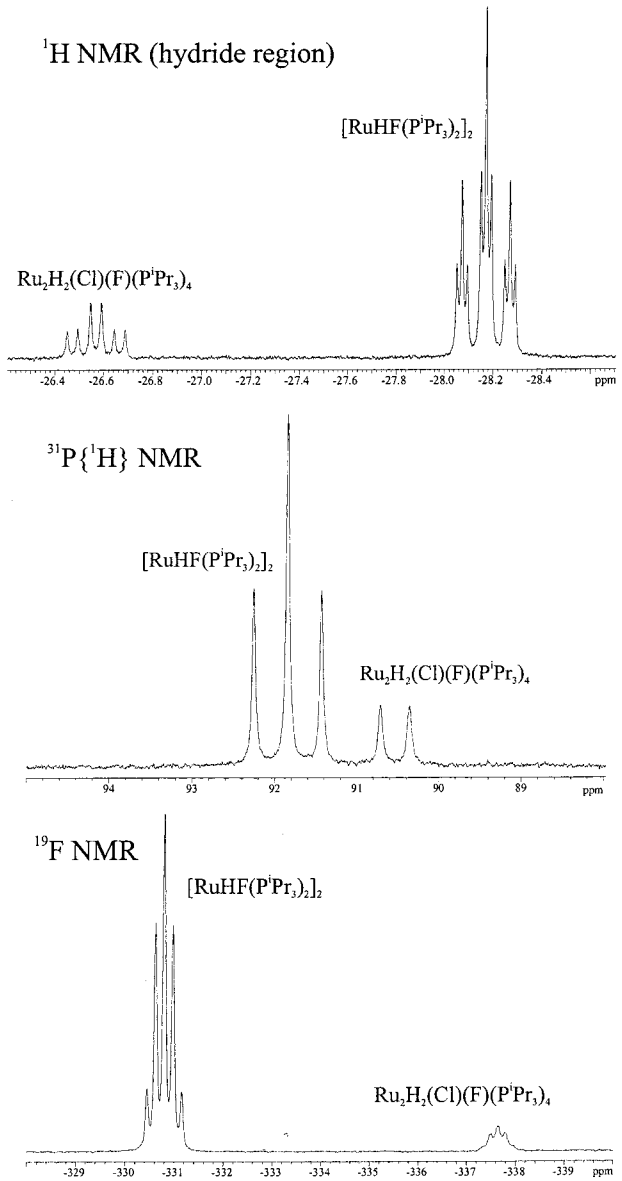

Figure 2. NMR spectra of a 1:4 mixture of $Ru_2(H)_2(Cl)(F)(P^iPr_3)_4$ and $[RuHF(P^iPr_3)_2]_2$.

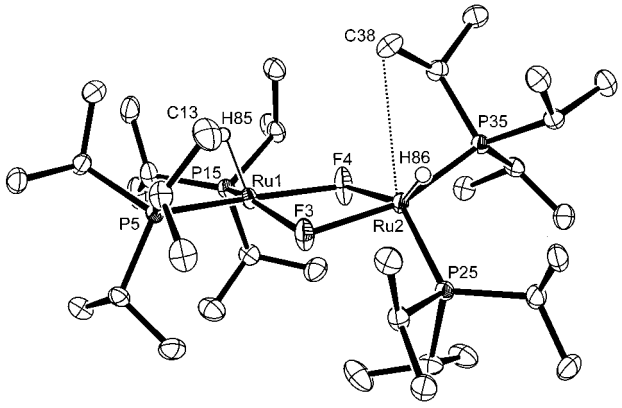

Figure 3. ORTEP drawing of $[RuHF(P^iPr_3)_2]_2$, showing selective atom labeling and the shortest Ru−C contacts (Ru2−C38 at 3.28 Å and Ru1−C13 at 3.49 Å). Hydrides are shown, but ^{i}Pr hydrogens are not.

2.21 ppm (m, 1H, P(C*H*Me$_2$)$_3$) and δ 1.26 (dd, 6H, P(CH*Me*$_2$)$_3$) and no resolvable ^{31}P{^{1}H} signal from extreme peak broadening. The lack of virtual coupling indicates cisoid phosphines in solution. As the temperature is lowered, two broad peaks are seen in the ^{31}P spectrum at 0 °C centered at δ 72.6 and 97.1 ppm that continue to decoalesce until sharpening occurs near −80 °C, with the peaks centered at δ 64.7 and 112.5 ppm. Several small ^{31}P signals also appear in this region at this low temperature, which are most likely the result of rotamers from hindered rotation of the phosphine ^{i}Pr substituents. By ^{1}H NMR, signals from the phosphines simply broaden upon temperature lowering and provide no structural information, but at −30 °C, a broad hydride appears at δ −13.5 ppm (bridging Ru*H*). When the temperature is further lowered, a second broad hydride appears with *twice* the intensity of the first at −80 °C and δ −24.2 ppm (terminal Ru*H*). As expected, several very small hydride signals also appear at this low temperature corresponding to the rotamers seen in the low-temperature ^{31}P NMR spectra.

Table 3. Selected Bond Distances (Å) and Angles (deg) for $[RuHf(P^iPr_3)_2]_2$

Ru(1)	P(5)	2.2385(7)	Ru(2)	P(35)	2.2394(7)
Ru(1)	P(15)	2.2276(7)	Ru(2)	F(3)	2.1292(15)
Ru(1)	F(3)	2.1130(15)	Ru(2)	F(4)	2.1148(15)
Ru(1)	F(4)	2.1121(15)	Ru(1)	H(a)	1.44(3)
Ru(2)	P(25)	2.1891(7)	Ru(2)	H(b)	1.56(3)

P(5)	Ru(1)	P(15)	106.584(26)	P(35)	Ru(2)	F(4)	92.58(5)
P(5)	Ru(1)	F(3)	92.50(5)	F(3)	Ru(2)	F(4)	74.20(6)
P(5)	Ru(1)	F(4)	166.40(4)	P(5)	Ru(1)	H(a)	80.2(11)
P(15)	Ru(1)	F(3)	153.93(5)	P(15)	Ru(1)	H(a)	80.2(12)
P(15)	Ru(1)	F(4)	87.02(5)	F(3)	Ru(1)	H(a)	121.3(12)
F(3)	Ru(1)	F(4)	74.58(6)	F(4)	Ru(1)	H(a)	102.7(11)
P(25)	Ru(2)	P(35)	107.355(27)	P(25)	Ru(2)	H(b)	78.9(11)
P(25)	Ru(2)	F(3)	90.90(5)	P(35)	Ru(2)	H(b)	84.7(11)
P(25)	Ru(2)	F(4)	135.23(6)	F(3)	Ru(2)	H(b)	98.6(11)
P(35)	Ru(2)	F(3)	161.73(5)	F(4)	Ru(2)	H(b)	144.1(11)

The presence of three hydrogens in the dimer $Ru_2(H)_3Cl(P^iPr_3)_4$ is confirmed by derivatization using N_2. After 30 min under 1 atm of N_2 in C_6D_6, two products are seen in a 1:1 ratio. One is identified as $RuHCl(N_2)(P^iPr_3)_2$ (**1**) by comparison with an authentic sample obtained from direct reaction of $[RuHCl(P^iPr_3)_2]_2$ with N_2.[6] The other product is identified as $Ru(H)_2(N_2)_2(P^iPr_3)_2$ (**2**) from the observation of a ^{31}P{^{1}H} NMR signal at 70.1 ppm, with integration intensity equal to that of **1**, and a new hydride signal (−13.3 ppm, broad) with *twice* the intensity of **1**'s hydride. The infrared spectrum of **2** in toluene shows *two* ν(NN) bands, thus proving the presence of two N_2 ligands. The observed frequencies, 2125 and 2163 cm^{-1}, lie within 1 cm^{-1} of those reported,[7−10] for $Ru(H)_2(N_2)_2(PCy_3)_2$, further confirming the identity of this product.

The X-ray study (Figure 4 and Table 4) shows that the entire molecule is the crystallographic asymmetric unit. The chloride is bridging, and the Ru_2ClP_4 unit has an idealized C_2 axis containing Cl and bisecting the Ru−Ru vector. This symmetry includes the unequal Ru−P bond lengths (as in $Ru_2H_2X_2(P^iPr_3)_4$) of 2.32 Å (to P4 and P24) and 2.21 Å (to P14 and P34); this symmetry also extends to the three methine carbons on each P, as well as to most of the methyl carbons. Three hydridic hydrogens were also located in a difference Fourier map but not refined. One is terminal on each metal, and the third bridges the two metals. Each Ru is thus five-coordinate. The two terminal hydrogens conform to the C_2 symmetry of the heavy

(6) Coalter, J. N.; Bollinger, J. C.; Huffman, J. C.; Werner-Zwanziger, U.; Caulton, K. G.; Davidson, E. R.; Gérard, H.; Clot, E.; Eisenstein, O. *New J. Chem.* **2000**, *24*, 9.
(7) Sabo-Etienne, S.; Hernandez, M.; Chung, G.; Chaudret, B.; Castel, A. *New J. Chem.* **1994**, *18*, 175.
(8) Oliván, M.; Caulton, K. G. *Inorg. Chem.* **1999**, *38*, 566.
(9) Belderrain, T.; Grubbs, R. H. *Organometallics* **1997**, *16*, 4001.
(10) Christ, M. L.; Sabo-Etienne, S.; Chung, G.; Chaudret, B. *Inorg. Chem.* **1994**, *33*, 5316.

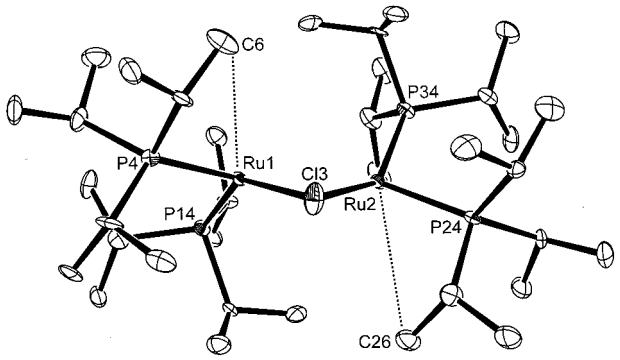

Figure 4. ORTEP drawing of the nonhydrogen atoms of $Ru_2H_3Cl(P^iPr_3)_4$ showing selected atom labeling. The shortest Ru−C contacts (Ru1 to C6 at 3.50 Å and Ru2 to C26 at 3.51 Å) are indicated.

Table 4. Selected Bond Distances (Å) and Angles (deg) for $Ru_2H_3Cl(P^iPr_3)_4$

Ru(1)	Cl(3)	2.4066(27)		Ru(2)	Cl(3)	2.4134(27)	
Ru(1)	P(4)	2.3210(28)		Ru(2)	P(24)	2.324(3)	
Ru(1)	P(14)	2.2104(26)		Ru(2)	P(34)	2.2144(28)	
Ru(1)	H(A)	2.13		Ru(2)	H(A)	1.92	
Ru(1)	H(B)	1.50		Ru(2)	H(C)	1.96	
Cl(3)	Ru(1)	P(4)	93.41(9)	P(14)	Ru(1)	H(A)	70
Cl(3)	Ru(1)	P(14)	138.31(10)	P(14)	Ru(1)	H(B)	77
P(4)	Ru(1)	P(14)	106.04(10)	H(A)	Ru(1)	H(B)	111
Cl(3)	Ru(2)	P(24)	92.76(9)	Cl(3)	Ru(2)	H(A)	94
Cl(3)	Ru(2)	P(34)	141.99(10)	Cl(3)	Ru(2)	H(C)	124
P(24)	Ru(2)	P(34)	105.86(10)	P(24)	Ru(2)	H(A)	147
Ru(1)	Cl(3)	Ru(2)	75.45(8)	P(24)	Ru(2)	H(C)	60
Cl(3)	Ru(1)	H(A)	89	P(34)	Ru(2)	H(A)	87
Cl(3)	Ru(1)	H(B)	144	P(34)	Ru(2)	H(C)	93
P(4)	Ru(1)	H(A)	176	H(A)	Ru(2)	H(C)	89
P(4)	Ru(1)	H(B)	67				

atom skeleton, which supports the credibility of their location. The bridging hydrogen lies slightly off the C_2 axis, but we believe this displacement is not real; its deviation is not statistically significant. The shorter Ru−P distances are those to phosphines, which are approximately trans to an empty coordination site, and the longer Ru−P distances are those to phosphines approximately *trans* to the μ-H. While it is challenging to assign a coordination geometry to Ru when several of the ligands are imperfectly located, and two ligands are very bulky (the P−Ru−P angles are quite small, at 106°), it is approximately square-pyramidal with apical P14 (or P34). One ^{i}Pr group of the basal atoms P4 and P24 then each shows one ∠Ru−P−C (105°) that is at least 6°−17° smaller than any other ∠Ru−P−C in the molecule. The resulting shortest Ru−C(H_3) distances are 3.50 Å (on P4) and 3.51 Å (on P24). Rather than being truly agostic, this probably only represents tucking the bulky group into a void in the square-pyramid geometry (i.e., trans to P14 and P34). The Ru−Ru separation is 2.95 Å, which is short because of the bridging hydride.

$Ru_2HCl_3(P^iPr_3)_4$. A single crystal X-ray diffraction study shows a structure best interpreted as two square pyramids connected by a shared basal edge (Figure 5 and Table 5). The only uncertainty is the location of the hydride ligand on Ru2, either at site a or at site b in **B**. It is noteworthy that, despite

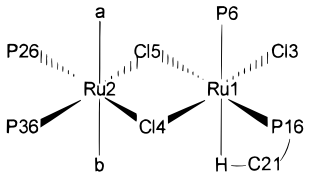

B

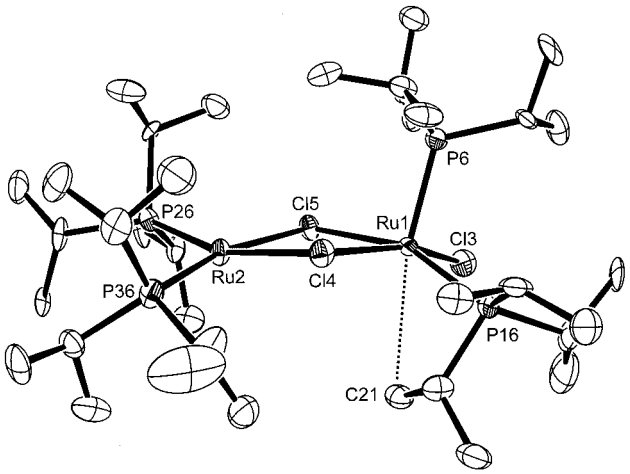

Figure 5. ORTEP drawing of the nonhydrogen atoms of $Ru_2HCl_3(P^iPr_3)_4$, showing selected atom labeling. The shortest Ru−C contact (to C21) is indicated.

Table 5. Selected Bond Disatances (Å) and Angles (deg) for $Ru_2HCl_3(P^iPr_3)_4$

Ru(1)	Cl(3)	2.380(3)		Ru(2)	Cl(4)	2.474(3)	
Ru(1)	Cl(4)	2.403(3)		Ru(2)	Cl(5)	2.474(3)	
Ru(1)	Cl(5)	2.466(3)		Ru(2)	P(26)	2.267(3)	
Ru(1)	P(6)	2.239(3)		Ru(2)	P(36)	2.278(3)	
Ru(1)	P(16)	2.304(3)					
Cl(3)	Ru(1)	Cl(4)	161.65(9)	P(6)	Ru(1)	P(16)	105.71(11)
Cl(3)	Ru(1)	Cl(5)	89.40(9)	Cl(4)	Ru(2)	Cl(5)	76.93(8)
Cl(3)	Ru(1)	P(6)	96.13(11)	Cl(4)	Ru(2)	P(26)	160.41(10)
Cl(3)	Ru(1)	P(16)	92.42(11)	Cl(4)	Ru(2)	P(36)	90.52(10)
Cl(4)	Ru(1)	Cl(5)	78.41(8)	Cl(5)	Ru(2)	P(26)	89.73(9)
Cl(4)	Ru(1)	P(6)	98.75(10)	Cl(5)	Ru(2)	P(36)	165.15(10)
Cl(4)	Ru(1)	P(16)	93.82(10)	P(26)	Ru(2)	P(36)	104.34(10)
Cl(5)	Ru(1)	P(6)	96.16(10)	Ru(1)	Cl(4)	Ru(2)	102.51(9)
Cl(5)	Ru(1)	P(16)	157.72(9)	Ru(1)	Cl(5)	Ru(2)	100.73(9)

the bulk of P^iPr_3, this molecule has *cis* phosphines; the P−Ru−P angles are only 104.3(1)° and 105.7(1)°. The apical Ru1−P6 distance (2.239(3) Å) is shorter than the three Ru−P(basal) distances (2.267(3)−2.304(3) Å), and the Ru(1)−Cl(4) distance *trans* to chloride (2.403(3) Å) is significantly shorter than the three Ru−(μ-Cl) distances *trans* to phosphines (2.466(3)−2.474(3) Å), consistent with the *trans* influence ranking of P and of Cl. When they are five-coordinate, both ruthenium centers are unsaturated. Ru(1) manifests this by accepting an agostic interaction from the C21−H bond of an ^{i}Pr methyl on P16 (Ru1−C21 = 3.02 Å). The next shortest distance is Ru2−C28, at 3.66 Å. To achieve this agostic interaction, the angle Ru(1)−P16−C20 decreases to 96.5(3)°; this is a reduction of over 13° compared to the next smallest value and is an unusually reliable indication of agostic bonding, given that X-ray diffraction does not reliably locate hydrogen atoms. The *absence* of any agostic interaction at Ru2 is fully consistent with the presence of a hydride at site a or site b, since the strong *trans* influence of hydride renders the empty coordination site on Ru2 a very weak acceptor. Judging by the direction of fold along the Cl5−Cl4 line, site a is the more likely site for the hydride. The Ru−Ru separation is 3.81 Å, which is nonbonding.

(η^5-C_6H_5O)RuH(P^iPr_3)$_2$. This compound was prepared in good yield by metathesis of $[RuHCl(P^iPr_3)_2]_2$ with TlOPh. The noninnocent nature of the phenoxide substituent is shown in the η^5-coordination mode adopted[11,12] by the arene ring rather than an η^1 oxygen linkage. The ^{1}H and ^{13}C{^{1}H} NMR data show

(11) Kuznetsov, V. F.; Yap, G. P. A.; Bensimon, C.; Alper, H. *Inorg. Chim. Acta* **1998**, *280*, 172.

Scheme 1

$$1/2\ [RuHFL_2]_2 + TMS\text{-}OSO_2R \xrightarrow[-\ TMS\text{-}F]{C_6H_6} [RuH(OSO_2R)L_2]_x \xrightarrow{C_6H_6} [(\eta^6\text{-}C_6H_6)RuHL_2]^+[OSO_2R]^-$$

$R = CF_3, CH_3$ — observed only for $R = CH_3$ — $R = CF_3$ - <5 min; $R = CH_3$ - hours

that the best description of this binding mode is as a cyclohexadienonyl anion (**III**−**VI**) from the upfield shifts (relative

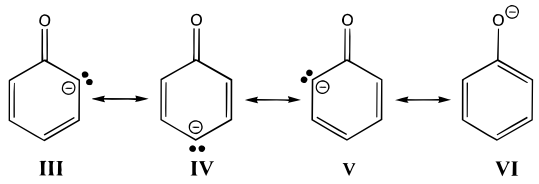

III **IV** **V** **VI**

to aromatic signals) of the phenoxide nonquaternary carbons and their accompanying protons. This binding mode is confirmed by the large downfield ^{13}C chemical shift of the carbon bound to oxygen (166 ppm), thus consistent with significant carbonyl character. The downfield shift of the hydride by ^1H NMR (−13.2 ppm) relative to signals characteristic of four- or five-coordinate unsaturated ruthenium species is in agreement with an η^5 binding mode, resulting in a coordinately saturated product.

Reactivity: Impact of Cl → F Transposition on Carbene Formation. We briefly compared the presence of F (vs Cl) on the ability of $[RuHX(P^iPr_3)_2]$ to isomerize ethyl vinyl ether to form a carbene ligand.[1] The reaction (eq 2) proceeds much more

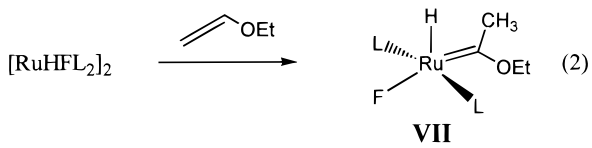

$[RuHFL_2]_2$ + OEt → (2)

VII

slowly (8 h half-life at 20 °C in benzene-d_6) when X = F perhaps because cleavage of the fluoride bridges by the vinyl ether is much slower than in the chloride-bridged dimer. During the reaction no intermediates are observed at ambient temperature by ^1H or ^{31}P NMR spectroscopy. The product (**VII**) has spectral features similar to those of its chloride analogue but with the added presence of ^{19}F coupling to the hydride (16 Hz) and phosphorus (24 Hz) nuclei. The ^{19}F NMR chemical shift of −228 ppm is consistent with a metal-bound fluoride. This carbene product reacts, on a time scale only somewhat slower than its formation, to produce $RuHF(CO)(P^iPr_3)_2$. While this is consistent with the general tendency of Ru to extract CO from aldehydes, alcohols, and even carboxyl compounds, the fate of the lost CH_3 and CH_2CH_3 was not established.

Reactivity: Fluoride Replacement Reactions. The fluoride ligand of $[RuHF(P^iPr_3)_2]_2$ is readily replaced by other anions X using Me_3Si-X. Reaction with both trimethylsilyl trifluoromethanesulfonate (TMS−OTf) and trimethylsilyl methanesulfonate (TMS−OSO_2Me) form, in the time of mixing, $[RuH(OSO_2R)(P^iPr_3)_2]_x$ (R = CF_3, CH_3) with liberation of trimethylsilyl fluoride. The same species (R = CF_3) is also obtained by treatment of $[RuHClL_2]_2$ with TMS−OTf. Both of these products transform, in benzene solution, to cationic arene complexes $[(C_6H_6)RuH(P^iPr_3)_2][OSO_2R]$ but at dramatically different rates (Scheme 1). With R = CF_3, this transformation takes only seconds to minutes, thus $[RuH(OTf)(P^iPr_3)_2]_x$ is never observed by NMR at room temperature. However, with R = CH_3, complete conversion to the arene complex takes several hours and $[RuH(OSO_2CH_3)(P^iPr_3)_2]_x$ can be characterized by solution spectroscopy. The degradation of these sulfonate complexes precludes analysis by X-ray crystallography so that their molecularity is uncertain. However, it is likely that the reluctance of these sulfonates to bridge two metals is the reason that benzene complexation occurs. When ethyl vinyl ether is added to a freshly prepared sample of $[RuH(OSO_2Me)(P^iPr_3)_2]_x$ in C_6D_6, immediate formation of the carbene complex $RuH(OSO_2Me)(P^iPr_3)_2(=C(Me)OEt)$ is observed by NMR spectroscopy (eq 3). $[RuHF(P^iPr_3)_2]_2$ also reacts rapidly with 2-trime-

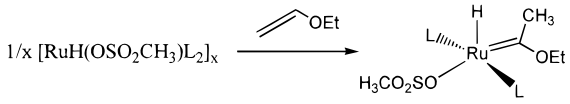

$1/x\ [RuH(OSO_2CH_3)L_2]_x$ + OEt → (3)

thylsiloxypent-2-ene-4-one to deliver the acetylacetonate (acac) ligand in quantitative yield (eq 4). The equivalent methyl and

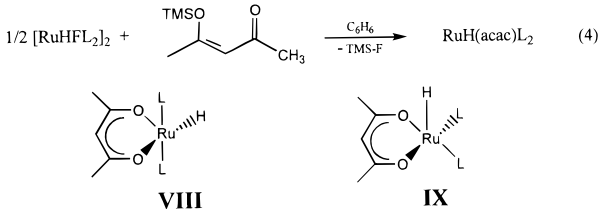

$1/2\ [RuHFL_2]_2$ + TMSO, O, CH_3 $\xrightarrow[-\ TMS\text{-}F]{C_6H_6}$ $RuH(acac)L_2$ (4)

VIII **IX**

carbonyl carbons of the acac moiety seen by ^{13}C NMR at room temperature do not exclude structure **VIII**, which could exhibit dynamic averaging of these signals in this unsaturated five-coordinate product, although **IX** is wholly consistent with the observed spectroscopic data. This square-pyramidal geometry was established[13] by X-ray diffraction for the isoelectronic Rh(III) vinyl complex $Rh(acac)(CH=CHR)(PCy_3)_2^+$. The bidentate nature of the acac ligand does *not*, however, prevent the isomerization of ethyl vinyl ether to a coordinated carbene (eq 5). The carbene product exhibits inequivalent methyl and

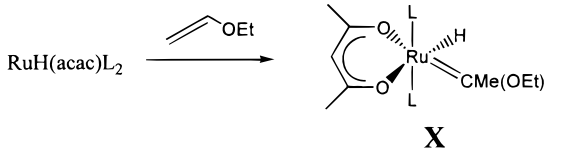

$RuH(acac)L_2$ + OEt → CMe(OEt) (5)

X

carbonyl signals by ^{13}C NMR, consistent with the illustrated six-coordinate structure. The chemical shift of C(α), 301 ppm, confirms the presence of a carbene substituent.

Formation of **X** is much slower than with $[RuHClL_2]_2$, taking 24 h for completion. It has been proposed that this transformation,[1] in which the hydride ligand is a catalyst, requires a reactive site *cis* to this hydride. This slow reaction rate is consistent with structure **IX** for $RuH(acac)(P^iPr_3)_2$, where the acac ligand must adopt an η^1 coordination mode either after vinyl ether com-

(12) Cole-Hamilton, D. J.; Young, R. J.; Wilkinson, G. *J. Chem. Soc., Dalton Trans.* **1976**, 1995.

(13) Esteruelas, M. A.; Lahoz, F. J.; Oñate, E.; Oro, L. A.; Rodríguez, L.; Steinert, P.; Werner, H. *Organometallics* **1996**, *15*, 3436.

plexation or in a slow preequilibrium before coordination to meet this requirement.

Discussion

This work shows the delicate balance between the achievability of 14-electron, four-coordinate Ru(II) for $RuR(CO)(P^tBu_2Me)_2^+$ (R = H, Ph) and dimerization of analogous species containing P^iPr_3 and halides. Presumably, the dimerization occurs because P^iPr_3 is less bulky than P^tBu_2Me, because halide is a much better bridging ligand than H or Ph, and also because the H, Ph, and CO ligands exert a sufficiently strong *trans* influence (in contrast to Cl) to discourage dimerization via any ligand trans to themselves. The small (105−106°, compared to their usual trans stereochemistry) ∠P−M−P values repeatedly observed here show the ability of two phosphines as large as P^iPr_3 to become cisoid.[14] This is important because cisoid phosphines are necessary for linking two square pyramids using basal−basal ligands (**C**). Linkage through apical−basal ligands

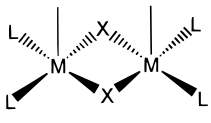

C

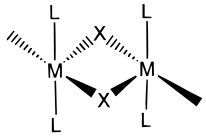

D

(**D**), while it leaves phosphine trans on each metal, involves repulsive end-to-end L−L contacts. It therefore is reasonable that we find dehydrohalogenation of $Ru(H)_2Cl_2(P^tBu_2Me)_2$ or $Ru(H)_2Cl_2(PCy_3)_2$ fails to cleanly produce "$RuHCl(P^tBu_2Me)_2$" or "$RuHCl(PCy_3)_2$". The use of these bulkier phosphine leads to unappealing product mixtures exhibiting many ^{31}P NMR signals.

The structures reported here show frequent adoption of square-pyramidal coordination geometry but often low symmetry (e.g., inequivalent Ru in a dimer and inequivalent P on one Ru). The progression of $Ru_2H_nCl_{4-n}(P^iPr_3)_4$ ($n = 1-3$) shows that bridging chloride is favored over bridging hydride, apparently because of the higher formal electron donor number of Cl vs H. Because the Ru−Ru separation is so different for two chlorides (3.71 Å) and two fluorides (3.35 Å) as bridges, we suggest this distance is controlled by mechanical factors (shorter Ru−F distances) and that any Ru−Ru bond is insignificant.

Although this work reveals that four-coordinate, monomeric $RuHX(P^iPr_3)_2$ is not isolable, the dimer shows typical behavior of $M_2(\mu\text{-}Cl)_2$ units: facile halide bridge splitting by Lewis bases, such as vinyl ethers and those as weak as N_2.[1,6]

It should be noted that all these structures, square pyramids fused at their basal edges, are those deduced from NMR data (**E**) for $[RuCl_2(PPh_3)_2]_2$.[15] The Ru−C "contacts" discussed above

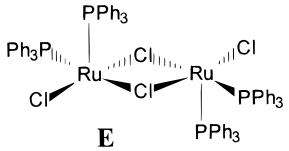

E

for every compound lack two features found[16] in a cationic dimeric Ru(II) complex of the ligand $^tBu_2PCH_2P^tBu_2$: truly short (2.51−2.57 Å) Ru−C distances and NMR inequivalence of the ^{t}Bu methyl groups. Consequently, the contacts reported here only manifest either very weak donation or mere space filling. This (in comparison to P^tBu_2Me) is consistent with P^iPr_3 being less bulky than P^tBu_2Me and that agostic interactions to R′ in this class of molecules depend[17] in part on the pendant R group bulk in PR_2R'.

These dimers have stoichiometry similar to that of $[RuHCl(^tBu_2PCH_2P^tBu_2)]_2$[16] reported recently. That dimer has bridging halides and one terminal hydride on each metal, the hydrides do not migrate between the metals, and the Ru−Ru separation is 3.239(1) Å. That dimer differs from those reported here in having a structure (**F**) with four equivalent Ru−P distances.

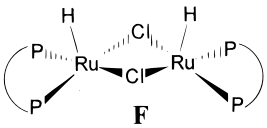

F

This is in best agreement with a structure also based on two square pyramids sharing a basal−basal edge.

Acknowledgment. This work was supported by the ACS PRF.

Supporting Information Available: One crystallographic file, in CIF format. This material is available free of charge via the Internet at http://pubs.acs.org.

IC991112Y

(14) Haas, C. M.; Nolan, S. P.; Marshall, W. J.; Moloy, K. G.; Proek, A.; Giering, W. P. *Organometallics* **1999**, *18*, 474.

(15) Hoffman, P. R.; Caulton, K. G. *J. Am. Chem. Soc.* **1975**, *97*, 4221.

(16) Hansen, S. M.; Rominger, F.; Metz, M.; Hofmann, P. *Chem. Eur. J.* **1999**, *5*, 557.

(17) Ujaque, G.; Cooper, A. C.; Maseras, F.; Eisenstein, O.; Caulton, K. G. *J. Am. Chem. Soc.* **1998**, *120*, 361.